



Significant step towards efficient electrical discharge machining titanium alloys

Ming Zhou¹ · Tianshang Hu¹ · Xin Mu¹ · Meng Zhao¹ · JianweiYang¹ · Qing Ye¹ · Pei Xu² · Lei Yang² · Fangqing Xin²

Received: 26 January 2023 / Accepted: 10 June 2023 / Published online: 22 June 2023
© The Author(s), under exclusive licence to Springer-Verlag London Ltd., part of Springer Nature 2023

Abstract

There have been high demands of high-quality, highly efficient processing methodologies on “difficult-to-cut” titanium alloys. The current methods for dealing with this kind of materials are mainly mechanical cutting ones. However, because of high processing costs, poor surface qualities, and restrictive machining operations, the costs of mechanical cutting methods are high. Electrical discharge machining (EDM), because of its flexibility, was considered as a supplement. However, serious difficulties arose while machining titanium alloys by EDM. Because of low thermo-conductivity of titanium alloys, the liquid temperature in gap between electrode and workpiece rose quickly after a series of pulse discharges. The high temperature of gap liquid usually led to gap liquid breakdown strength to decline. The consequence was discharging pulses tended out to be stable arc pulses or short pulses, burning workpiece surface and wearing electrode. The machining process became unstable. The low thermal conductivity of titanium alloys was the inherent property which could be hardly changed, and at present, the only way to settle the hard-to-cut problem of machining titanium alloys by EDM was to seek a way to keep gap liquid breakdown strength not go down so fast but still be suitable for effective pulse discharges. To solve this problem, this paper first listed three conditions to be met and analyzed the reasons to affect gap liquid breakdown strength in detail and concluded with three factors, gap distance, amount of chips left in gap, and gap liquid deionization after pulse discharges and then came up with a proposition to the problem. Technically, the proposition was accomplished by constructing a multiple-variable adaptive control system in which gap servo-voltage proportional to gap distance was in charge of discharging extent of pulses, electrode-discharging time decided the amount of chips produced in an electrode discharging cycle, and pulse-off time decided gap liquid deionization after discharges. These variables were timely regulated to keep the liquid breakdown strength suitable for discharging and meanwhile avoiding arcing in machining. The verification test demonstrated that the multivariable control system really helped electrical discharge machining titanium alloys in severe machining situations and proved its usefulness in applications.

Keywords Electrical discharge machining (EDM) · Multivariable adaptive control · Titanium machining · Liquid breakdown strength

Nomenclature

$\tau_{\text{deleterious}}$	An accumulated number of stable arc pulses and short pulses	$y_m(t)$	Machining state
$\tau_{\text{effective}}$	An accumulated number of spark pulses and transient arc pulses	ϑ	Machining state stable interval
τ_{delay}	An accumulated number of delay pulses	y_{me}	Machining state expectancy
		$y_e(t)$	Gap environment state
		$y_{ee}(t)$	Gap environment state expectancy
		$e_i(t), i = 1, 2$	Parameter estimation errors of EDM process and gap environment models
		$\theta_i, i = 1, 2$	Parameter vectors of EDM process and gap environment models
		$\hat{\theta}_i(t), i = 1, 2$	Estimated parameter vectors of EDM process and gap environment models
		$U_{sv}(t)$	Gap servo-voltage at time t
		$\hat{y}_i(t+2 t), i = 1, 2$	2-step ahead estimations of gap state $y_i(t+2)$ at time t , $y_1(t+2) = y_m(t+2)$, $y_2(t+2) = y_e(t+2)$

✉ Ming Zhou
zhouming@bucea.edu.cn

¹ Beijing Key Laboratory of Performance Guarantee on Urban Rail Transit Vehicles, School of Mechanical Electronic and Vehicle Engineering, Beijing University of Civil Engineering and Architecture, Beijing, China

² AECC Aviation Power Co., LTD., Xi'an, China

1 Introduction

Titanium alloys, known as light metal materials of the 21st century, have attracted many attentions in aircraft, atomic energy, marine, and medical equipment industries because of excellent mechanical, chemical, and other properties of titanium alloys [1]. However, titanium alloys are difficult-to-cut materials for traditional machining technics to fabricate them effectively and economically because of high melting points around 1400–1600°C and low elasticity modules of titanium alloys, and it may become even worse when the shapes of work parts interfere with tool paths [2]. The rapid accumulation of cutting heat results in poor dimensional accuracies and surface integrities of the workpiece [3].

Due to the low specific heat coefficient and thermal conductivity of titanium alloys, the rapid increase of local temperature during processing also led to rapid wear of a tool and reducing its service life. At the same time, because the elastic modulus of titanium alloy was low, it was easy to produce strong friction between tool and workpiece, which intensified tool's wear and reduced processing quality [4]. The strong alloying tendency or chemical reactivity of titanium alloys with most tool materials caused wear, welding, and smearing of machining tools on interacting surfaces, leading to rapid destructions of tool overcutting or premature failures and poor surface finishes [5]. Therefore, many researchers had been looking for effective methods to process titanium alloys through unconventional processing techniques [6].

Electrical discharge machining (EDM) relies on pulse discharges between electrodes to generate a certain amount of heat, 10,000°C–12,000°C, which melts and vaporizes machined surface materials and removes chips, the separated materials from the workpiece, out of gap between electrode and workpiece [7]. Meanwhile, that an electrode and a workpiece in working do not directly contact each other in machining thereby eliminates the mechanical stress, chatter, and vibration problems during a machining process and alleviates the difficulties due to the low elasticity modules in machining titanium alloys.

Scholars using EDM have conducted numerous studies on titanium alloys. Wang et al. [8] researched an EDM fuzzy control system to carry out machining micro-hole on titanium alloy material. The results showed that the method improved the stability and efficiency of the process. Vibro-assisted EDM was helpful to develop more efficient deep slot EDM. This is proved by Tsai et al. [9], and they found that the material removal rate of vibro-assisted EDM was better than that of non-vibro-assisted EDM with copper and copper-tungsten electrodes. Yu et al. [10] proposed a high-efficiency and high-quality EDM and atomic machining combined process that first uses graphite electrode EDM to machine titanium alloys and then used abrasive flow

machining (AFM) to polish the machined surface. This method greatly improved the surface quality of the small group of holes in the titanium alloy by EDM and improved the processing efficiency. Gu et al. [11] studied a way of EDM processing titanium alloys with bundled die-cutting electrodes. The feasibility of strapping electrodes for processing titanium alloys was studied, and the effect of solid die-cutting electrodes on EDM performance was compared. Wang et al. [12] proposed a new type of ultra-high-speed electric discharge machining, milling, and arc composite machining titanium alloy; this method, as reported, could machine difficult-to-machine materials efficiently.

The studies mentioned above, as reported, had improved EDM performance in machining titanium alloys. However, from the perspective of EDM mechanism, narrow gap distances and high discharging frequencies of EDM coupled with the low heat conductivity of titanium alloy often led to a fast rise of temperature in gap local liquid after pulse discharges. High temperatures in gap might cause local dielectric liquid breakdown strength decrease and the deionization of dielectric liquid incomplete after discharges. If that happened, it was highly possible that next pulses penetrated at this area of the decreased liquid breakdown strength and the discharging pulses afterwards turned out to be arcing pulses, damaging the machined workpiece surface and wearing electrode, and even worse, the process became unstable. Therefore, really solving the hard-to-cut problem by EDM needed to study from the crux of the mechanism and improve EDM operation. Specifically, the key to improving the poor machining stability is to find ways of keeping gap liquid breakdown strength suitable for efficient discharging and meanwhile avoiding arcing pulses in machining.

Avoiding gap liquid to lose its breakdown strength in gap in a machining process was a prerequisite and essential condition for stably machining titanium alloys by EDM. This paper first analyzed in detail the reasons of making gap liquid breakdown strength decline in machining and then came up with a proposition to keep gap liquid breakdown strength strong while in machining. Finally, put forward a feasible way, that is, to build a multivariable adaptive control system greatly increasing EDM Tool operational functions to accomplish the proposition. To be specific, three variables in an EDM Tool, namely, gap servo-voltage which was proportional to gap distance, electrode-discharging time which decided the amounts of debris produced per electrode discharging cycle, and pulse-off time which was crucial for gap liquid deionization after pulse discharges, were selected for the purpose. To keep gap liquid breakdown strength in machining titanium alloys, the three control variables had to be timely regulated to reach an appropriate gap distance, suitable amounts of debris accumulated in gap, and a proper pulse-off time for complete liquid deionization after pulse discharges.

The technically proposed scheme of a multivariable adaptive control system provided an effective way as a methodology in machining titanium alloys. The innovation approach exhibited overwhelmingly advantages over the commonly used EDM Tools in machining titanium alloys, mainly on the aspects of operation stableness with no side flushing and with no human attendance, high machining efficiency, and low electrode wear. Meanwhile, the methodology in this paper also provided an idea of solving the problems of severe tool wear, high machining costs, etc. which were the bottlenecks restricting the high-efficiency and high-quality cutting of titanium alloy parts for decades.

This paper was organized as follows. Section 1 gives the introduction. Section 2 gives a detailed analysis of the influential factors towards liquid breakdown strength. Section 3 technically proposes a multiple-variable adaptively control system to help electrical discharge machining titanium alloys. Section 4 verifies the feasibility of electrical discharging titanium alloy aided by the multivariable adaptive control system. Section 5 provides conclusions.

2 Analysis of gap liquid breakdown strength in machining titanium alloys

In an electrical discharge machining (EDM) process, there are five kinds of discharging pulses in gap, shown in Fig. 1: spark pulses, transient-arc pulses, stable-arc pulses, short pulses, and open pulses. In these pulses, open pulses are not discharging pulses. Spark pulse is a discharging pulse with a special feature of delay time, transient-arc pulse also is a discharging pulse with little delay time and discharges with voltage variations of high frequency, stable-arc pulse is a discharging pulse with little delay time and voltage variations of reduced frequencies, and short pulse is a discharging pulse as well whose voltage is the lowest among discharging pulses with voltage variations of further reduced frequencies. The interval between two discharge pulses is called pulse-off time whose function is to deionize the gap liquid after pulse discharges. Spark pulses and transient-arc pulses

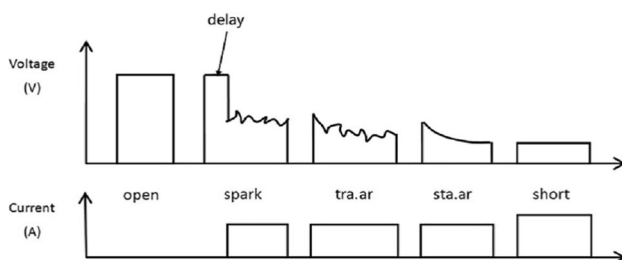


Fig. 1 Five kinds of discharging pulses

are effective discharge pulses, while stable-arc pulses and short pulses are deleterious discharge pulses, generally called arcing pulses. Pulses were discriminated by comparing sampled gap voltage and current with thresholds through pulse discrimination criteria [13].

2.1 Conditions of machining titanium alloys

Because titanium is an active metal element, it combines with the carbon element decomposed from heated dielectric fluid by local high-temperature workpiece surface in gap to form titanium carbide (TiC) in subsurface layer of the workpiece [14]. Because the melting point of TiC is 3150 °C, it is difficult to melt and remove the combination and thus hinders the EDM process [15]. Therefore, it is suggested to adopt positive polarity machining titanium alloys that the positive of Tool power is connected to workpiece instead of commonly used negative polarity machining, because the heat generated by electron bombarding workpiece surface is much less than the heat generated by positive ion bombarding workpiece surface. In this case, little titanium carbide (TiC) is formed in processes.

Condition 1: workpiece is connected to the positive of Tool power and electrode is connected to the negative of Tool power so that the created amounts of TiC combination are little since the heat generated by electron bombarding the workpiece surface is greatly less than the heat generated by positive ion bombarding the workpiece surface.

The raised high temperature of the gap local liquid by molten part of workpiece surface often makes liquid deionization of the local discharge area incomplete after pulse discharges, because of the low thermo-conductivity feature of titanium alloys, if pulse-off time is not long enough. From experiments in machining titanium alloys, it is suggested to set pulse-off time n times longer than the time of the pulse-on time.

Condition 2: in a stable and efficient machining process, the deionization is a prerequisite for the machining and it must be sufficient or complete.

Dielectric liquid breakdown strength in gap is not a constant but kept on changing in machining. When the strength is strong enough, most of discharging pulses are effective discharge pulses. When the strength lowers to some extent due to the increased amount of chips in gap, discharging pulses become arcing pulses, and the machining has to be stopped. Therefore, the liquid breakdown strength is a decisive factor in machining.

Condition 3: the breakdown strength in gap must be maintained properly in efficient and stably machine titanium alloys.

Condition 1 and condition 2 are easy to be met, and condition 3 is the key to stably and efficiently machining titanium alloys.

2.2 Analysis of gap liquid breakdown strength

1. Essentially, the breakdown strength of the dielectric liquid in gap determined what kinds of discharging pulses in gap.

If the breakdown strength of gap liquid is strong, most of discharging pulses are spark pulses. If the breakdown strength of the dielectric liquid is medium, most of discharging pulses are transient arc pulses; and if the breakdown strength of the dielectric liquid is weak, most of the discharging pulses are stable arc pulses or short pulses. Therefore, the liquid breakdown strength in machining is the key to determine the kinds of discharging pulses in gap.

2. The breakdown strength of the dielectric liquid is mainly affected by three factors, namely, gap distance, the amount of chips accumulated in gap, and the extent of liquid deionization in gap after discharges.

1. Gap distance is a main factor to determine gap dielectric liquid breakdown strength. A long gap distance ensures the dielectric liquid breakdown strength strong, and it is difficult for pulses to penetrate the gap. The pulses in the gap are mainly open pulses or spark pulses with relatively long delay times or both kinds. A medium-sized distance also means a lowered liquid breakdown strength. The pulses are mainly spark pulses with a little delay time or transient arc pulses or both kinds. A further lowered gap distance often leads to transient arc pulses or stable arc pulses or short pulses depended on the specific dielectric liquid breakdown strength in gap. Therefore, what kinds of pulses or a specific ratio of any kind of discharging pulses in a time can be obtained by adjusting gap distance. In other words, gap distance decides the discharging extent of pulses.
2. If gap distance is unchanged in machining in an electrode discharging cycle, gap liquid breakdown strength is still changing in an electrode-discharging cycle, because chips are produced in the electrode-discharging time of the cycle, which is a main part of electrode discharging cycle in Fig. 2. Most of the chips produced are moved out of gap by explosion forces of pulse discharging and electrode retraction movements. The ever-increasing amount of chips in gap in the electrode-discharging time directly lowers gap liquid breakdown strength on the assumption that gap liquid deionization is complete after pulse discharges. In this case, electrode-discharging time is a determinate factor to decide the amount of chips left in gap; in other words, electrode-discharging time is a crucial factor as well to decide gap liquid breakdown strength. Gap environment state below refers to the gap liquid breakdown strength at the end of electrode-discharging time.
3. Gap liquid deionization is a process of recovery from gap liquid ionized state after discharges of a pulse to

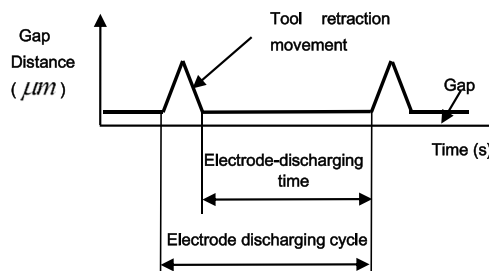


Fig. 2 Schematic illustration of tool discharging cycle

liquid deionization state in the period of pulse-off time. A pulse cycle is composed of pulse-on time and pulse-off time. It is obviously seen in Fig. 3 that after each discharging pulse there is a negative gap voltage at the beginning of pulse-off time. The negative gap voltage specifies the ionized gap liquid. When gap voltage reaches zero in the end of pulse-off time, the deionization of gap liquid is complete; if gap voltage does not reach zero in the end of pulse-off time, the deionization of gap liquid is incomplete. Most of the gap voltages recover from the negative to zero in pulse-off times, as shown in Fig. 3. However, there are two examples of incomplete liquid deionization, indicated in Fig. 3. The incomplete liquid deionization also decreases the breakdown strength of gap liquid. The consequence of incomplete liquid deionization is that the followed discharging pulse increases the possibility to be a transient arc pulse or an arc pulse or a stable arc pulse. So, incomplete gap liquid deionization decreases liquid breakdown strength.

3. Electrode-discharging time determines the amounts of chips produced in an electrode discharging cycle and thereafter decides gap environment situation, gap distance ensures the discharging extent of a pulse and decides pulse-discharging efficiencies, and pulse-off time guarantees gap liquid deionization which is the prerequisite for EDM. Amount of chips in gap, gap distance, and gap liquid deionization, put together, determine gap liquid breakdown strength. Since it is difficult to measure gap distance but gap distance is proportional to gap servo-voltage, gap distance measurement can be replaced by measurement of gap servo-voltage. In other words, electrode-discharging time which decides the amount of chips in gap is in charge of gap environment situation, gap servo-voltage which is in charge of discharging extent of pulses, and pulse-off time which is in charge of gap liquid deionization can be employed and timely controlled together to obtain suitable liquid breakdown strengths for a stable and efficient process in machining titanium alloys.

Proposition: Tool parameters, electrode-discharging time, gap servo-voltage, and pulse-off time, selected as control variables, must be timely adjusted for maintaining a

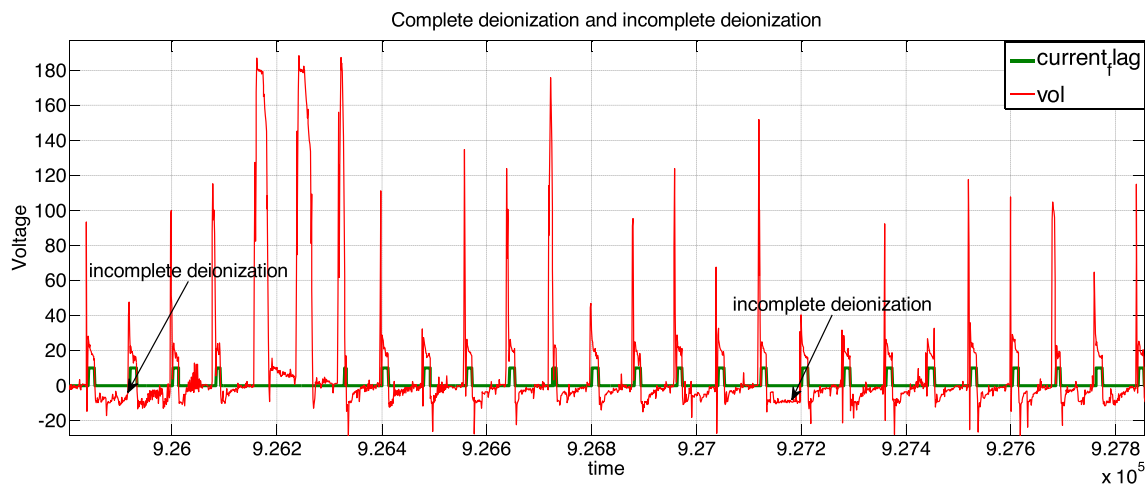


Fig. 3 Gap liquid complete and incomplete deionization after discharges

proper liquid breakdown strength for an efficient machining process and in the meantime avoiding arcing pulses.

An adaptive control system could accomplish this proposition. Therefore, a multiple-variable adaptive control system had to be built in this regard.

3 Multiple-variable adaptive control system

3.1 Machining indexes

Definition 1: machining state $y_m(t)$ at time t is defined to be a ratio of the number of deleterious discharging pulses to the number of whole pulses in a series of discharging pulses.

A small machining state $y_m(t)$ signifies that most of discharging pulses are spark pulses with long delays. A larger machining state $y_m(t)$ signifies that most of discharging pulses are spark pulses with little delays, or transient arc pulses, or both in gap. A further large machining state $y_m(t)$ signifies that most of discharging pulses are stable arc pulses, or short pulses, or both. From Definition 1, machining state $y_m(t)$ is a statistical index to quantify the kinds of pulses and discharging extent of pulses. Therefore, a machining process can be digitalized by a series of machining states.

A stable interval is defined to be

$$\vartheta_1 = (0, \epsilon_1), \epsilon_1 < 1. \tag{1}$$

Because different materials have different melting points, the values of ϵ_1 in machining different materials are different and determined by experiments. A machining is stable when machining state $y_m(t)$ is in the interval ϑ , $y_m(t) \in \vartheta_1$; the machining becomes unstable, machining state $y_m(t)$ is out of it and at this time arcing pulses

dominate in gap. Therefore, to maintain a stable and fast machining, machining state $y_m(t)$ has to be restricted in ϑ_1 .

A gap environment state is a machining situation in the end of electrode-discharging time, quantified breakdown strength of gap liquid. If a gap environment state is a large one indicating that the dielectric liquid is easy to be penetrated and the gap environment is not fit for the machining because, it is highly possible that discharging pulses are mostly arcing pulses in this gap environment. If a gap environment state was small, it indicates that gap environment is fit for the machining and most of discharging pulses are spark pulses or transient arc pulses. Further explorations of machining processes reveal that gap environment is strongly correlated with machining states and thereby the state of gap environment should be derived from machining states.

Definition 2: gap environment state $y_e(t)$, a quantified gap environment, is defined to be a correlation function of current and previous machining states $y_m(t), y_m(t-1), \dots, y_m(t-m)$,

$$y_e(t) = f_{\text{corr}}(y_m(t), y_m(t-1), \dots, y_m(t-m)) \tag{2}$$

where $y_m(t-m)$ denotes a machining state at time $t-m$.

Gap environment also refers to the workability of the dielectric liquid in the gap. As there is a stable interval ϑ_2 for machining state $y_m(t)$, correspondingly, there is also a rational interval. A stable interval of gap environment is defined to be

$$\vartheta_2 = (0, \epsilon_2), \epsilon_2 < 1. \tag{3}$$

The values of ϵ_2 in machining different materials are different and determined by experiments. ϵ_2 is the upper limit of the interval out of which gap environment is not fit for machining where arcing pulses dominate the gap and machining is unstable. A machining process was fit for

machining when gap environment state $y_e(t)$ is in the interval ϑ_2 , $y_e(t) \in \vartheta_2$. The larger the gap environment state $y_e(t)$ is in the rational interval ϑ_2 , the weaker is the breakdown strength of dielectric liquid and the more easily a pulse penetrates the gap and vice versa; and the process becomes worse when gap environment state $y_e(t)$ is out of it. Therefore, to maintain a sound machining process, gap environment state $y_e(t)$ has to be restricted in ϑ_2 .

3.2 EDM process model and gap environment model

An EDM process had been proven to be definite a non-linear process [16]. This process could be approximated by a timely linear model in which the structure of the model was linear, but the parameters of the model were timely varying with time in machining [17]. In an EDM process, many factors will influence machining situations. These factors are mainly divided into internal factors and external factors. Internal factors include power setting and machine servo setting; the former includes pulse current, pulse voltage, and pulse-on time. The latter includes gap servo-voltage, pulse-off time, electrode discharge-time, electrode jumping speed, and height. External factors include different electrode materials and workpiece materials, machined depths, discharging positions, and flushing conditions.

Both EDM process model and gap environment model consisted of a deterministic part and a random part. An impulse transfer function described the deterministic part and a transfer function which was a filtered white noise described the random part [17].

An EDM process mathematical model was

$$y_m(t) = \frac{B_{m1}(q)}{A_{m1}(q)}u(t) + \frac{C_{m1}(q)}{D_{m1}(q)}e_1(t) \tag{4}$$

where q is a forward shift operator, $A_{m1}(q)$, $B_{m1}(q)$, $C_{m1}(q)$, and $D_{m1}(q)$ are polynomials of q , $A_{m1}(q) = 1 + a_{m1}q^{-1} + \dots + a_{mn_a}q^{-mn_a}$, $B_{m1}(q) = b_{m1}q^{-1} + b_{m2}q^{-2} + \dots + b_{mn_b}q^{-mn_b}$, $C_{m1}(q) = 1 + c_{m1}q^{-1} + \dots + c_{mn_c}q^{-mn_c}$, and $D_{m1}(q) = 1 + d_{m1}q^{-1} + \dots + d_{mn_d}q^{-mn_d}$, and in this EDM process model, $e_1(t)$ is a white noise with zero mean and variance σ_1^2 [16].

An EDM environment mathematical model was

$$y_e(t) = \frac{B_{e1}(q)}{A_{e1}(q)}u(t) + \frac{C_{e1}(q)}{D_{e1}(q)}e_2(t) \tag{5}$$

where q was a forward shift operator, $A_{e1}(q)$, $B_{e1}(q)$, $C_{e1}(q)$, and $D_{e1}(q)$ were polynomials of q , $A_{e1}(q) = 1 + a_{e1}q^{-1} + \dots + a_{en_a}q^{-en_a}$, $B_{e1}(q) = b_{e1}q^{-1} + b_{e2}q^{-2} + \dots + b_{en_b}q^{-en_b}$, $C_{e1}(q) = 1 + c_{e1}q^{-1} + \dots + c_{en_c}q^{-en_c}$, and $D_{e1}(q) = 1 + d_{e1}q^{-1} + \dots + d_{en_d}q^{-en_d}$, and in this EDM process model, $e_2(t)$ is a white noise with zero mean and variance σ_2^2 .

Next, let the parameter vectors be

$$\theta_1 = [b_{m1} \dots b_{mn_b} \ a_{m1} \dots a_{mn_a} \ c_{m1} \dots c_{mn_c} \ d_{m1} \dots d_{mn_d}]^T \tag{6}$$

$$\theta_2 = [b_{e1} \dots b_{en_b} \ a_{e1} \dots a_{en_a} \ c_{e1} \dots c_{en_c} \ d_{e1} \dots d_{en_d}]^T \tag{7}$$

In order to minimize the weighted least squares criterion, we used the recursive least squares algorithm to estimate the parameters of the above polynomials [17],

$$\hat{\theta}_1(t) = \arg \min_{\theta_1} \sum_{k=1}^t \beta_1(t, k) [y_m(t)(k) - \varphi_1^T(k)\theta_1]^2 \tag{8}$$

$$\hat{\theta}_2(t) = \arg \min_{\theta_2} \sum_{k=1}^t \beta_2(t, k) [y_e(t)(k) - \varphi_2^T(k)\theta_2]^2 \tag{9}$$

$\hat{\theta}_i(t)$, $i = 1, 2$ were the vectors, which contained the estimate parameters of the polynomials in Eqs. (3) and (4), $\beta_i(t, k) = \lambda_i(t)^{t-k}$, $i = 1, 2$, $0 \leq k \leq t-1$, $\lambda_i(t)$, $i = 1, 2$, were forgetting factors and $\beta_i(t, t) = 1$, $\varphi_i(t)$, $i = 1, 2$, contained lagged input and output variables.

The timely parameters of the process model, in Eqs. (4) and (5) were recursively estimated by least-square algorithm [18],

$$\begin{cases} \hat{\theta}_i(t) = \hat{\theta}_i(t-1) + L(t)[y_i(t)(t) - \varphi_i^T(t)\hat{\theta}_i(t-1)] \\ L_i(t) = \frac{P_i(t-1)\varphi_i(t)}{\lambda_i(t) + \varphi_i^T(t)P_i(t-1)\varphi_i(t)} \\ P_i(t) = \frac{1}{\lambda_i(t)} \left[P_i(t-1) - \frac{P_i(t-1)\varphi_i(t)\varphi_i^T(t)P_i(t-1)}{\lambda_i(t) + \varphi_i^T(t)P_i(t-1)\varphi_i(t)} \right] \end{cases} \quad i = 1, 2 \tag{10}$$

where $y_1(t) = y_m(t)$, $y_2(t) = y_e(t)$.

Both models could be used for online applications. The two models in Eqs. (4) and (5) were further simplified as

$$A_m(q)y_m(t) = B_m(q)u_1(t) + C_m(q)e_1(t) \tag{11}$$

where $A_m(q) = A_{m1}(q)D_{m1}(q)$, $B_m(q) = B_{m1}(q)D_{m1}(q)$, and $C_m(q) = A_{m1}(q)C_{m1}(q)$; and

$$A_e(q)y_e(t) = B_e(q)u_2(t) + C_e(q)e_2(t) \tag{12}$$

where $A_e(q) = A_{e1}(q)D_{e1}(q)$, $B_e(q) = B_{e1}(q)D_{e1}(q)$, and $C_e(q) = A_{e1}(q)C_{e1}(q)$.

3.3 Control laws

The prime role of gap distance is to determine the discharging extent of a pulse which directly influences machining efficiency and stableness in machining. At present, it is unpractical to measure gap distance in dielectric liquid, especially timely varied gap distances in a process. However, the value of gap servo-voltage is linearly proportional to a gap distance. In this case, gap servo-voltage can be used to replace gap distance to decide the discharging extent of a pulse.

Definition 3: machining state expectancy y_{me} is defined to be an ideal machining state that governs pulse discharging extents, as well as a machining stableness, $y_{me} \in \vartheta_1$, and $y_{me} < \epsilon_1$.

In a machining process, if machining state $y_m(t)$ rises over a defined machining state expectancy y_{me} , gap servo-voltage which determines gap distance, then increases to a calculated value, leading to an enlarged gap distance to lower discharging extents of pulses. Machining state $y_m(t)$ is then forced to decrease. Conversely, if machining state $y_m(t)$ is lower than the defined machining state expectancy y_{me} , gap servo-voltage then decreases to a calculated value, leading to a shortened gap distance to increase discharging extents of pulses. Machining state $y_m(t)$ is then forced to increase. In this way, machining state $y_m(t)$ fluctuates around a machining state expectancy y_{me} . The machining state expectancy y_{me} has to be selected properly so that machining state y_m , fluctuating around the machining state expectancy y_{me} , can be kept in the range ϑ_1 .

Lemma 1: gap servo-voltage $U_{sv}(t)$ performs the function to reduce the error between the machining state $y_m(t)$ and a machining state expectancy y_{me} . Then, it follows

$$\left\{ U_{sv}(t) : y_m(t) \propto \frac{K_1}{U_{sv}(t)} ; s.t(|y_m(t) - y_{me}| \rightarrow 0) \right\} \quad (13)$$

where K_1 is a constant.

Except that machining states are changing all the time in a machining process, gap environment is also changing because of the variation of dielectric liquid breakdown strength affected by the varied amount of chips left in gap. Most of the chips produced are moved out of gap by spark explosion forces and electrode retraction movements. The amount of chips left in gap affect dielectric liquid breakdown strength directly. More chips in gap cause the liquid breakdown strength decrease and vice versa. That is not to say that gap situation with no chips in gap is the best for machining. On the contrary, there is an optimal liquid breakdown strength for discharging or a certain amount of chips in gap. We call this gap environment situation “gap environment state expectancy” indexed by y_{ee} .

Definition 4: gap environment state expectancy y_{ee} is defined to be an ideal gap environment for a stable machining process, $y_{ee} \in \vartheta_2$, and $y_{ee} < \epsilon_2$.

In a machining situation, if gap environment is so harsh that environment state $y_e(t)$ is larger than expected environment state y_{ee} because of too many amounts of metal chips in gap resulting in liquid breakdown strength decreases, electrode-discharging time then decreases to produce less amounts of chips in a shortened discharging time. Under such circumstance, spark explode forces and higher frequent electrode withdraw movements than before together help moving produced chips out of gap more to

lessen the amount of chips in gap. Less amount of chips in gap ensures recovery of the liquid breakdown strength. Conversely, if gap environment is so fine that environment state $y_e(t)$ is smaller than an expected environment state y_{ee} because of less amounts of chips in gap resulting in liquid breakdown strength stronger, electrode-discharging time then elongates its discharging time to produce larger amounts of chips in gap to decrease the liquid breakdown strength in gap. In this way, gap environment state $y_e(t)$ fluctuated around gap environment state y_{ee} . In this way, gap liquid breakdown strength is maintained fit for a stable machining process.

Lemma 2: electrode-discharging time $T_{DN}(t)$ performs the function to reduce the error between the gap environment state $y_e(t)$ and a gap environment state expectancy y_{ee} . Then, it follows

$$\left\{ T_{DN}(t) : y_e(t) \propto K_2 * T_{DN}(t) ; s.t(|y_e(t) - y_{ee}| \rightarrow 0) \right\} \quad (14)$$

where K_2 is a constant.

Lemma 3: pulse-off time $T_{OFF}(t)$ performs the function to reduce the error between the machining state $y_m(t)$ and a machining state expectancy y_{me} . Then, it follows

$$\left\{ T_{OFF}(t) : y_m(t) \propto \frac{K_3}{T_{OFF}(t)} ; s.t(|y_m(t) - y_{me}| \rightarrow 0) \right\} \quad (15)$$

where K_3 is a constant.

Lemma 1 and Lemma 3 in Eqs. (13) and (15) are similar in form that gap servo-voltage and pulse-off time are all required to regulate according to machining state, but they perform different functions that gap servo-voltage is in charge of the discharging extent of a pulse and pulse-off time gap liquid deionization. Pulse-off time fluctuates as the same way as gap-servo-voltage does, but based on n times longer of a pulse-on time to guarantee the complete deionization of gap liquid after discharges.

Theorem: the control laws for the multivariate adaptive control system are derived by minimizing the variances of the errors of $(y_i(t+2) - \hat{y}_i(t+2|t))$,

$$u_i(t) = \frac{C_i}{B_i} y_{ie} + \frac{A_i - C_i}{B_i} y_i(t), i = 1, 2 \quad (16)$$

so that the errors are white noises with the variance σ_i^2 , $i = 1, 2$, where $i = 1$ refer to machining state, $y_1(t+2) = y_m(t+2)$ is the machining state at time $t+2$, $\hat{y}_1(t+2|t) = \hat{y}_m(t+2|t)$ is estimated two-step ahead machining state with the known machining state $y_m(t)$; $i = 2$ refer to gap environment state, $y_2(t+2) = y_e(t+2)$ is gap environment state at time $t+2$, $\hat{y}_2(t+2|t) = \hat{y}_e(t+2|t)$ is estimated two-step ahead gap environment state with the known gap environment state $y_e(t)$; $y_{1e} = y_{me}$, $y_{2e} = y_{ee}$.

Proof:

From Eqs. (3) and (4), if two-step ahead predictive control is adopted, $d_0 = \deg A_i - \deg B_i = 2$, it follows

$$\begin{aligned} y_i(t+2) &= \frac{q^2 B_i}{A_i} u_i(t) + \frac{C_i}{A_i} e_i(t+2) \\ &= \frac{q^2 B_i}{A_i} u_i(t) + e_i(t+2) + \frac{C_i - A_i}{A_i} e_i(t+2) \\ &= e_i(t+2) + \frac{q^2 B_i}{A_i} u_i(t) + \frac{q^2 (C_i - A_i)}{A_i} e_i(t) \end{aligned} \quad (17)$$

It can be obtained by Eqs. (11) and (12) that

$$e_i(t) = \frac{A_i}{C_i} y_i(t) - \frac{B_i}{C_i} u_i(t) \quad (18)$$

Substituting Eq. (18) into Eq. (17),

$$\begin{aligned} y_i(t+2) &= e_i(t+2) + \frac{q^2 B_i}{A_i} u_i(t) + \frac{q^2 (C_i - A_i)}{A_i} \left[\frac{A_i}{C_i} y_i(t) - \frac{B_i}{C_i} u_i(t) \right] \\ &= e_i(t+2) + \frac{q^2 B_i}{A_i} u_i(t) + \frac{q^2 (C_i - A_i)}{C_i} y_i(t) - \frac{q^2 B_i (C_i - A_i)}{A_i C_i} u_i(t) \\ &= \frac{B_i}{C_i} q^2 u_i(t) + \frac{q^2 (C_i - A_i)}{C_i} y_i(t) + e_i(t+2) \end{aligned} \quad (19)$$

Let

$$\hat{y}_i((t+2|t)) = \frac{B_i}{C_i} q^2 u_i(t) + \frac{q^2 (C_i - A_i)}{C_i} y_i(t) \quad (20)$$

Then,

$$y_i(t+2) = \hat{y}_i((t+2|t)) + e_i(t+2) \quad (21)$$

and let

$$\hat{y}_i((t+2|t)) = y_{ie} \quad (22)$$

From Eq. (20),

$$u_i(t) = \frac{B_i}{C_i} y_{ie} + \frac{A_i - C_i}{B_i} y_i(t) \quad (23)$$

and

$$y_i(t+2) - \hat{y}_i((t+2|t)) = e_i(t+2).$$

In summary, the error of $(y_i(t+2) - \hat{y}_i((t+2|t)))$ is white noise with variance σ_e^2 .

Pulse-off time $T_{OFF}(t)$ is regulated according to the varied machining state, the same way as gap servo-voltage does. Pulse-off time $T_{OFF}(t)$ is also required to be n times larger than pulse-on time T_{ON} in machining titanium alloys from condition 2. It followed

$$T_{OFF}(t) = n \times T_{ON} + k_4 \times U_{SV}(t) \quad (24)$$

where T_{ON} is a constant, k_4 is also a proportional constant.

3.4 Multivariable adaptive control system for EDM

A schematic diagram of the multivariable adaptive EDM is shown in Fig. 4. A machining state expectancy y_{me} is fed into the upper adaptive control system. The computed gap servo-voltage $U_{sv}(t)$ from the control law in Eq. (16) forces machining state $y_m(t)$ to approach machining state expectancy y_{me} so that the expected discharging extent of pulses can be obtained.

Theoretically, pulse-off time $T_{OFF}(t)$ is regulated according to machining state $y_m(t)$ as well, with the consideration of condition 2. Simply, pulse-off time $T_{OFF}(t)$ is got in Eq. (24).

A gap environmental state expectancy y_{ee} is fed into the lower adaptive control system. Likewise, the computed electrode discharging time $T_{DN}(t)$ from the control law in Eq. (16) forces environment state $y_e(t)$ to approach gap environment state expectancy y_{ee} , and the expected gap environment situation can be reached.

4 Verification test

A verification test was carried out to verify the performance of electrical discharge machining Ti-6Al-4V, aided by the multivariable adaptive control system. The experiment was to process a through-hole with a graphite electrode of diameter $\varnothing 16$ without side flushing and human attendance. The test was operated in a closed machining situation where the chips were moved out of gap only in upward direction in the whole machining process. Table 1 lists the electrode and workpiece measurements and requirements.

Machining parameter settings are listed in Table 2. The polarity was set negative from condition 1, and pulse-on time was set $80 \mu s$ for the consideration of machining efficiency in negative polarity. Because the electrode diameter was $\varnothing 16$ mm, the current was specifically set 30 A for the match, and pulse voltage was set 200 V for pulse easily penetrating gap. Electrode discharge time, gap voltage, and pulse off were selected as variables timely regulated in the process.

From Eq. (26), it was known that the variations of pulse_off were similar to the variations of gap servo-voltage, and so it was not necessary to show the variations of pulse_off in figures.

Figure 5 consisted 4 subplots. 1×1 subplot showed the variations of gap environment in the whole process, 2×1 subplots showed timely regulated electrode-discharging time in the whole process, 1×2 subplot showed the variations of machining states in the whole process, and 2×2 subplot showed the timely regulated the variations of gap servo voltage.

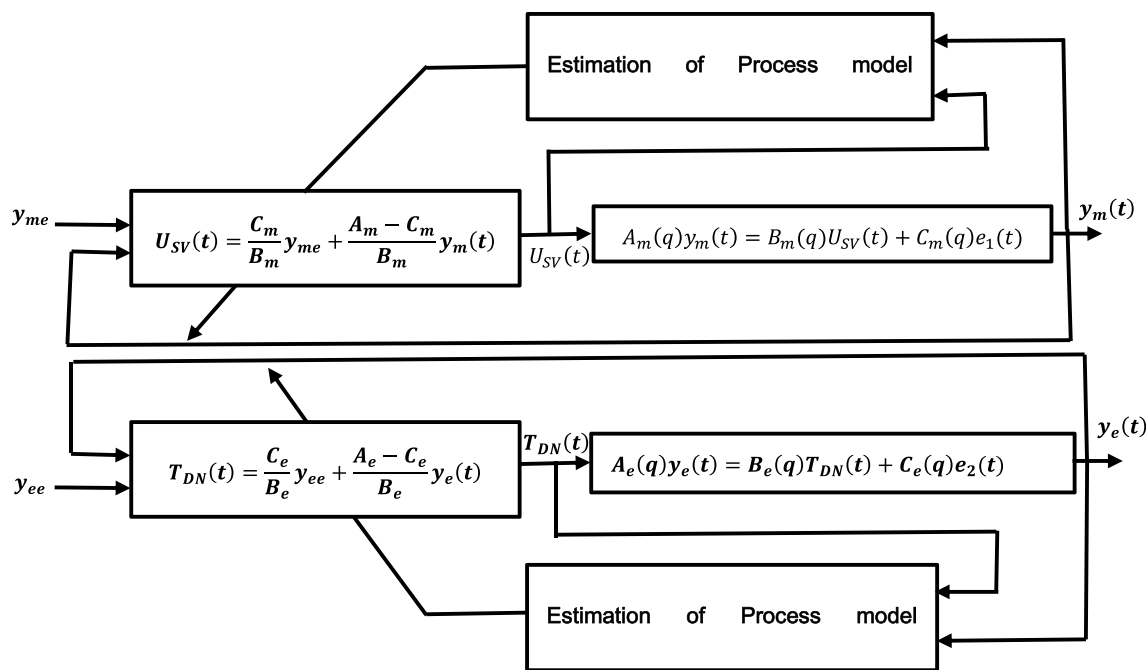


Fig. 4 Schematic diagram of EDM multivariate adaptive control system

Table 1 Electrode and workpiece measurements and requirements

Electrode (solid)	Electrode diameter (mm)	Length of work-piece (mm)	Requirements		
			Closed machining situation or open machining situation	Side flushing	Human attendance
Graphite	16	114	Closed	No	No

Table 2 Parameter settings of machining Ti-6Al-4V by adaptive servo-voltage

Pulse voltage (V)	Current (A)	Pulse_on time (μ s)	Polarity (electrode)
200	30	80	Negative

The gap environment state in this closed machining situation experienced huge distinctive variations from a healthy environment of few chips in gap at beginning to a hostile environment of too many chips left in gap in the end, because it was more and more difficult to move produced chips along upward direction out of the continuously deepened blind hole. To handle this kind of complex situation, it was suggested that gap environment state expectancy

y_{ee} had to be changed smaller after the machining experienced a length of distance so that input discharging energy could match up with machining environment. As shown in 1×1 subplot of Fig. 5, the entire process was roughly divided into four subprocesses by four different state expectancy $y_{ee1}, y_{ee2}, y_{ee3}$, and y_{ee4} . Because gap environment became more and more severe in machining, gap environment state expectancies had to be smaller in accordance, that was, $y_{ee1} > y_{ee2} > y_{ee3} > y_{ee4}$, to gradually lessen electrode-discharging times to produce less chips in order to maintain a proper liquid breakdown strength (healthy environment) for discharging.

The 1×2 subplot of Fig. 5 was a display of machining state variations in the process. Theoretically, machining state interval was $(0, 1]$, and gap servo-voltage interval was $(0-150]$. Practically, gap servo-voltage interval was set $[20, 150]$. If accumulated chips left in gap led to the decrease of gap liquid breakdown strength, the amplitude of the variations of machining state $y_m(t)$ which varied around machining state expectancy y_{me} to track it was likely to go beyond ϑ_1 . In this case, machining state expectancy y_{me} was suggested to lower down so that the amplitude of machining state $y_m(t)$ was still in the stable interval ϑ_1 . Therefore, machining state expectancy y_{me} had to be matched up with gap environment state expectancy y_{ee} . Likewise, in 1×2 subplot of Fig. 5, there were also four machining state expectancies $y_{me1}, y_{me2}, y_{me3}, y_{me4}$ in the four subprocesses, and $y_{me1} > y_{me2}, > y_{me3} > y_{me4}$. In this subplot, it was obvious that variations of machining state underwent from small values

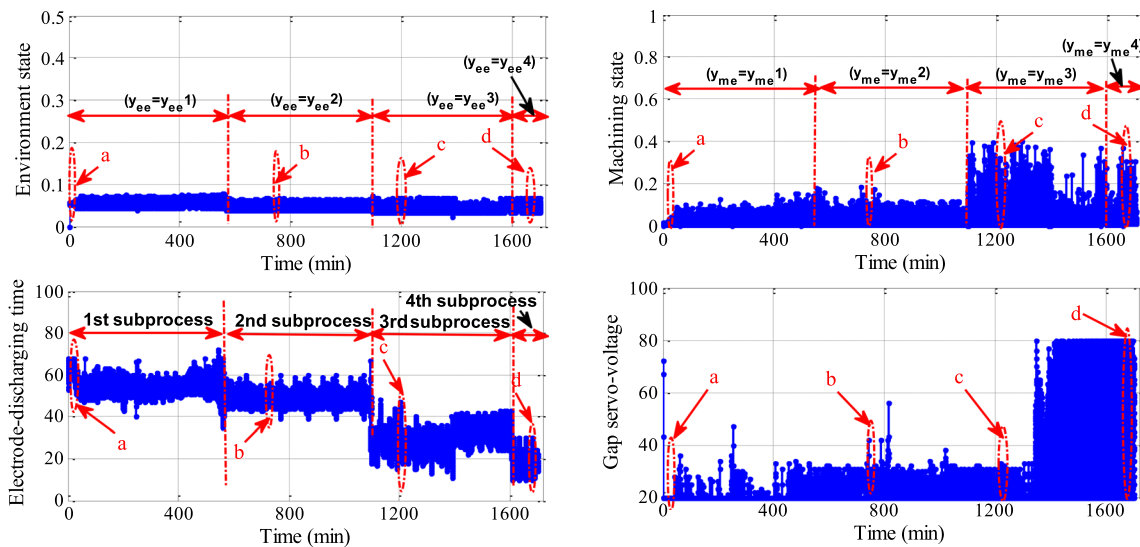


Fig. 5 The entire process of machining Ti-6Al-4V

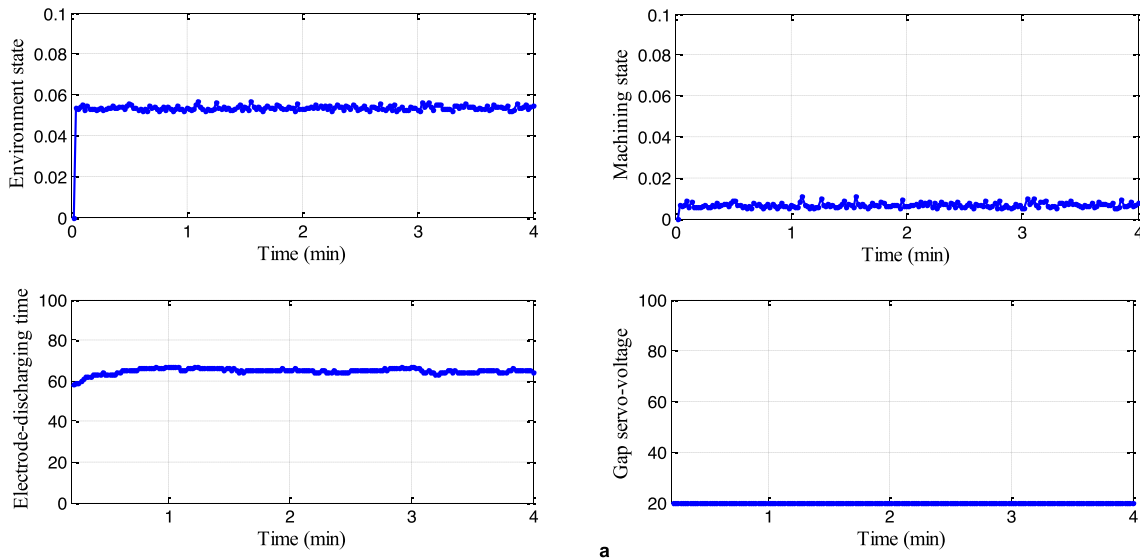


Fig. 6 Part a in the first subprocess

to large ones, but still in \mathcal{D}_1 . We specifically chose (a), (b), (c), (d) parts in four subprocesses for a clear exhibition. The 2×2 subplot of Fig. 5 was a display of gap servo-voltage values regulated to force machining state $y_m(t)$ to track machining state expectancy y_{me} .

Figure 6 shows the incipient stage of the process. At this stage, because it was easy to move chips out of gap, the gap liquid breakdown strength was strong. The environment state expectancy y_{ee} was chosen the largest y_{ee1} so that electrode-discharging time, shown in 1×2 subplot, was regulated in Eq. (16) according to the varied environment states in 1×1 subplot as large as it could to reach optimal machining environment. Electrode-discharging time varied in the range [60, 63].

Meanwhile, because machining state expectancy y_{me} was also chosen the largest one y_{me1} , gap servo-voltage was computed in Eq. (11) to be less than or equal to 20, the inferior limit of gap servo-voltage which practically decided the smallest gap distance. The smallest gap distance determined the highest discharging extents of pulses to increase machining state.

The largest electrode-discharging time, lowest gap servo-voltage, and smallest pulse-off time decided the highest machining efficiency in the process that was the steepest slope of machining-depth curve indicated in Fig. 6.

Figure 7 part b shows the detailed machining situation in the second subprocess in which environment state expectancy y_{ee} equaled to y_{ee2} and machining state expectancy

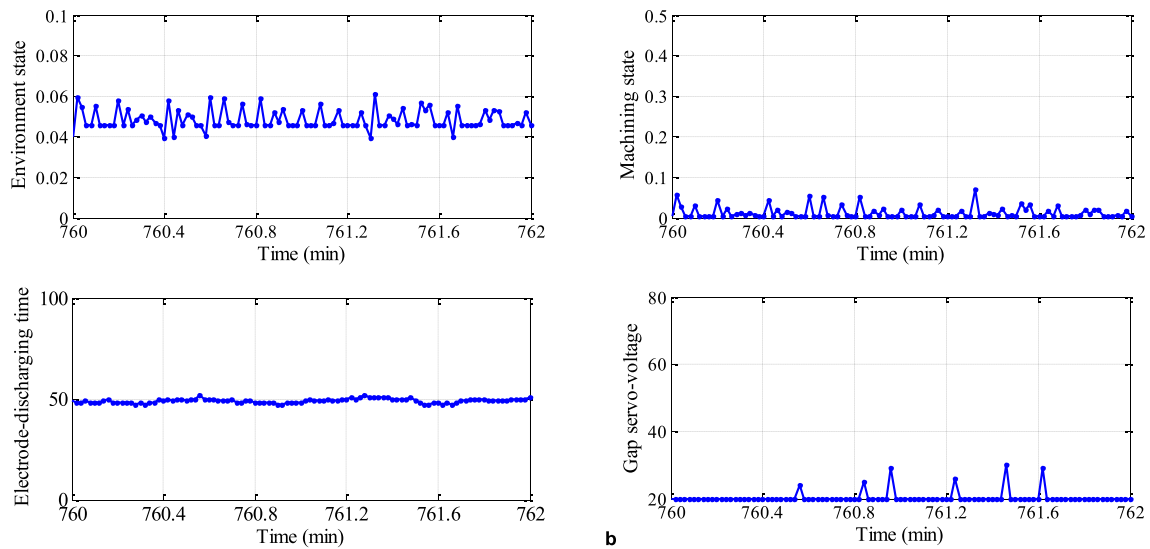


Fig. 7 Part b in the 2nd subprocess

y_{me} equaled to $y_{me}2$. As $y_{ee}2 < y_{ee}1$ and $y_{me}2 < y_{me}1$, less input discharging energy and smaller discharging extent of a pulse were required in the second subprocess than those in the first subprocess. In this case, electrode-discharging time was computed in the range [48 51], shown in 2×1 subplot, and there were a few gap servo-voltages larger than 20, though most of gap servo-voltages were computed still less or equal to 20 in the 2×2 subplot. The machining efficiency in this subprocess was a little slower than that in the first subprocess because of decreased electrode-discharging time and a few gap servo-voltages >20 . The decreased machining efficiency represented by the slope of machining-depth curve could be observed in the second subprocess less than the slope of machining-depth curve in the 1st subprocess.

In the 3rd subprocess, more and more chips left in gap resulting in gap liquid breakdown strength decrease, because it was difficult to move out the produced chips due to the long-machined distance. To keep the gap environment suitable for discharging, the input discharging energy represented by electrode-discharging time had to lessen to match up with the decreased liquid breakdown strength. Part c representatively showed machining situation in the 3rd subprocess. $y_{ee} = y_{ee}3 < y_{ee}2$ forced electrode-discharging time varying in the range [21, 35], shown in the 2×1 subplot of Fig. 8, which was much less than the range [48 51] in the 2×1 subplot of Fig. 8 for the decreased liquid breakdown strength. Though the variations of machining states in 1×2 of Fig. 8 were a little more violent than the variations of machining states in the 1×2 subplot of Fig. 8, it was still tolerable for the fact that most of gap servo-voltage were less than or equal to 20 in the 1×2 subplot of Fig. 8.

In the final subprocess, even more chips were left in gap because of even longer upward machined distance, leading

to gap liquid breakdown strength continuously decreased; the gap was easier to be penetrated by pulse voltages. However, $y_{ee} = y_{ee}4 < y_{ee}3$ forced electrode-discharging time varying in the range [17, 23] shown in the 2×1 subplot of Fig. 9 to input less discharging energy. In this case, the range of gap environment state variations changed little seen in the 1×1 subplots of Figs. 7, 8, and 9. In other words, gap environments were maintained well, suitable for machining, by adaptively regulating electrode discharging time according to the different gap environment state expectancies and varied gap environment states in different subprocesses. At this stage $y_{me} = y_{me}4 < y_{me}3$, the smallest machining state expectancies, among $y_{me}1, y_{me}2, y_{me}3, y_{me}4$, forced gap servo-voltage to enlarge to increase gap distance for lessening discharging extents of pulses. So, machining states were forced to keep in the stable interval ϑ_1 by adaptively regulating gap servo voltage.

Figure 10 depicts the machining depth with time. Considering the fact of unavoidable electrode wear in machining titanium alloy Ti-6Al-4V, the machining depth was set 135 mm though the machined depth of the through-hole was 114 mm. The slope of the machining depth curve $\tan\alpha$ represented the machining efficiency. In the 1st subprocess, there were two slopes, $\tan\alpha_1$ in 0–50 minutes and $\tan\alpha_2$ in 50–550 minutes. In the incipient stage 0–50 minutes, since both $y_{ee} = y_{ee}1$ and $y_{me} = y_{me}1$ were the largest, and produced chips were easy to be exploded out of gap by pulse discharges and electrode retraction movements, electrode discharging time was computed around 63 which was the largest in the process, gap servo-voltages computed less than or equal to 20 which was the smallest value, and pulse-off time was also the smallest from Eq. (26). On such an occasion, machining efficiency is the largest in the process. In Fig. 10, $\alpha_1 > \alpha_2 > \alpha_3 > \alpha_4 > \alpha_5$ demonstrated that machining efficiency

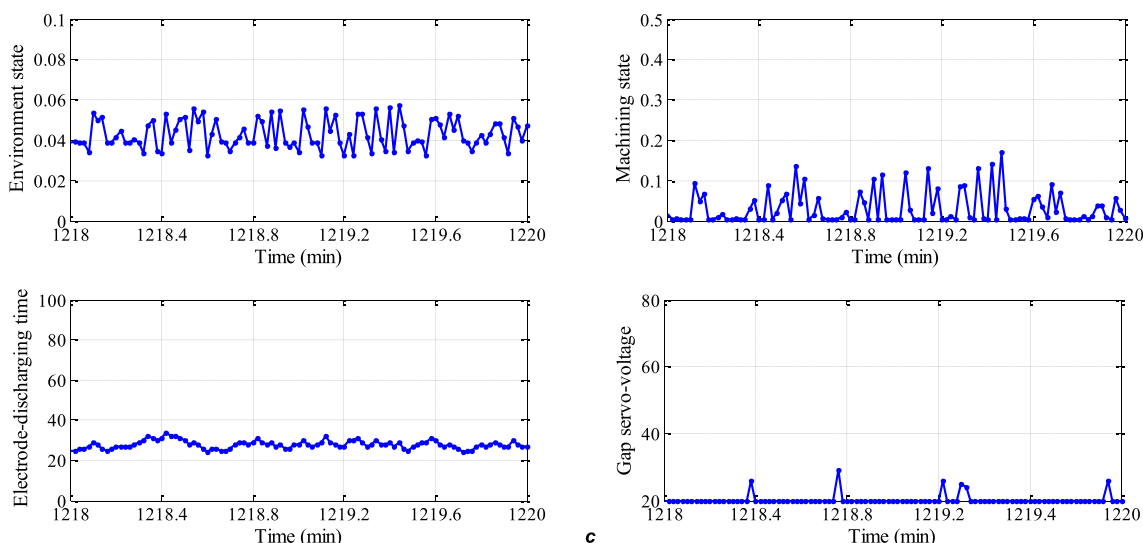


Fig. 8 Part c in the 3rd subprocess

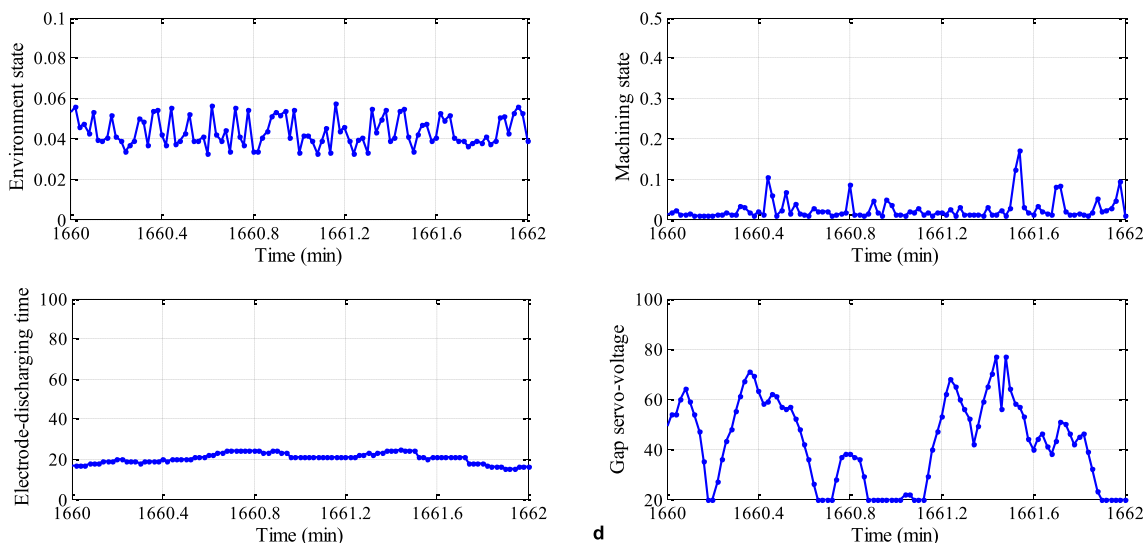


Fig. 9 Part d in the 4th subprocess

lowered as the machining depth of the blind hole deepened. However, except two machining efficiencies $\tan\alpha_1$ and $\tan\alpha_2$ in the 1st subprocess, the machining efficiency changed small in a subprocess followed.

Since the workpiece was connected to the positive of Tool power and the graphite electrode was connected to the negative of Tool power, electrode wear was unavoidable. After the through-hole was made, the electrode wear ratio was calculated to be

$$\begin{aligned}
 \text{Electrode wear ratio} &= \frac{\text{Volum}_{\text{worn-out of electrode}}}{\text{Volum}_{\text{machined of workpiece}}} \times 100\% \\
 &= \frac{5.268 \times 10^3}{24.317 \times 10^3} \times 100\% = 21.664\%
 \end{aligned}$$

Figure 11 shows the clamping of Ti-6Al-4V workpiece and the machined through-hole, cut apart by wired EDM. From Fig. 11, it could be seen that side discharges during the machining caused the actual size of the processed workpiece (16.48 mm) to be larger than the electrode size (16 mm). The machining capability of the system was verified through the 114 mm through-hole machining TC4 experiment. From the calculation results of the final machining time and electrode wears, it could be concluded that the established multivariable adaptive electric discharge machining control system could achieve efficient and low wear machining of titanium alloys.

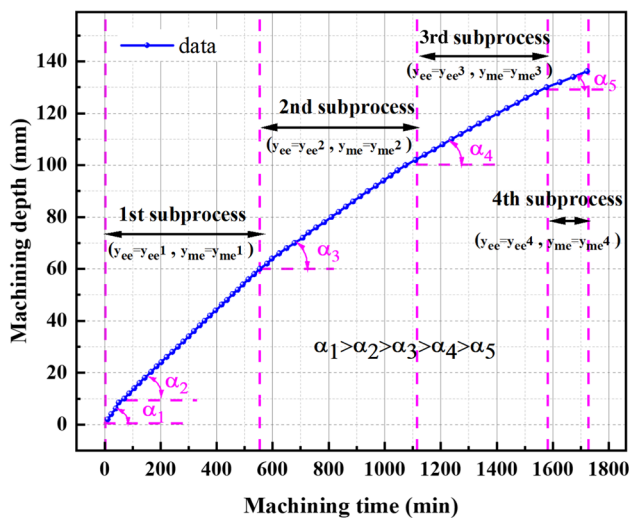
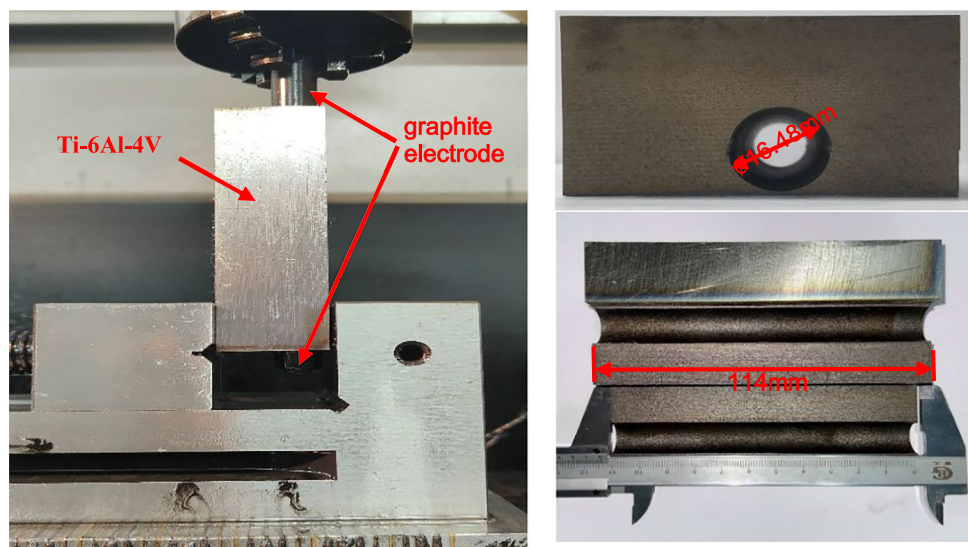


Fig. 10 Machined depth curve

Fig. 11 Machined through-hole cut apart by wired EDM



5 Conclusions

The main difficulty of machining titanium alloys by EDM is the fast rise of local liquid temperature in gap after pulse discharges due to the low specific heat coefficient and thermal conductivity of titanium alloys. The raised temperature of gap liquid usually leads to a decline of gap liquid breakdown strength which is the reason to cause arcing pulses in machining. The low thermal conductivity of titanium alloys is the inherent property which can be hardly changed, and the only way to settle the hard-to-cut problem by EDM is to seek a method to keep gap liquid breakdown strength not go down so fast but still be suitable for effective pulse discharges.

To this end, this paper listed three conditions to be met and came up with a proposition to machining titanium alloys

and innovatively created a multivariable adaptive control system to accomplish the proposition. Some major conclusions were listed below:

- (1) Gap liquid breakdown strength was the decisive factor in electrical discharge machining titanium alloys and affected by three factors, gap distance, chips left in gap, and gap liquid deionization after pulse discharges.

Gap distance determined the discharging extent of pulses. However, the gap liquid breakdown strength was still changing because of chips produced in gap in electrode-discharging time. Incomplete or complete gap liquid deionization after pulse discharges also influenced gap liquid breakdown strength.

- (2) It developed a new multivariable adaptive control system in which gap servo-voltage proportional to

gap distance decided the discharging extent of pulses, electrode-discharging time decided gap environment state which was directly affected by produced chips in gap, and pulse-off time decided the deionization of gap liquid after pulse discharges.

- (3) To testify EDM operation in machining titanium alloy Ti-6Al-4V aided by the newly developed multivariable adaptive control system, it machined a through-hole of 114 mm with the diameter 16 mm of a graphite electrode and with no side flushing and no human attendance. The machining was conducted in a closed machining situation in which generated chips were moved out only in upward direction. The machining efficiency did not change much in the whole process, and electrode wear ratio was 21.664%.

- (4) The machining results showed that the multivariable adaptive control system could help EDM to achieve high machining efficiency and low electrode wear. The problem of low conductivity of titanium alloys easily causing gap liquid breakdown strength decline was settled by the approach in this paper. This multivariable adaptive EDM system qualified for machining titanium alloys.

Author contribution Ming Zhou: conceptualization, methodology, software, visualization, writing—original draft. Tianshang Hu: investigation, data collection. Xin Mu: formal analysis. Meng Zhao: data curation. Jianwei Yang: resources. Qing Ye: writing—review and editing. Pei Xu: resources. Lei Yang: supervision. Fangqing Xin: validation.

Funding This research has been supported by “The Fundamental Research Funds for Beijing Universities (No. X18082) awarded to Ming Zhou,” “Beijing Education Committee Scientific Plan Foundation (No. 051101904) awarded to Ming Zhou,” “The Post Graduation Innovation Project of Beijing University of Civil Engineering and Architecture (PG2022122) awarded to Tianshang Hu,” and “The Post Graduation Innovation Project of Beijing University of Civil Engineering and Architecture (DG2022016) awarded to Xin Mu.”

Declarations

Competing interests The authors declare no competing interests.

References

- Kou ZJ, Han FZ, Wang GS (2019) Research on machining Ti6Al4V by high-speed electric arc milling with breaking arcs via mechanical-hydrodynamic coupling forces. *J Mater Process Technol* 271:499–509. <https://doi.org/10.1016/j.jmatprotec.2019.04.021>
- Mamedov A, Lazoglu I (2016) Thermal analysis of micro milling titanium alloy Ti–6Al–4V. *J Mater Process Technol* 229:659–667. <https://doi.org/10.1016/j.jmatprotec.2015.10.019>
- Zhao XL, Niinomi M, Nakai M, Ishimoto T, Nakano T (2011) Development of high Zr-containing Ti-based alloys with low Young’s modulus for use in removable implants. *Mater Sci Eng C* 31(7):1436–1444. <https://doi.org/10.1016/j.msec.2011.05.013>
- Liu Y, Zhang WC, Zhang SF, Sha ZH (2014) The simulation research of tool wear in small hole EDM machining on titanium alloy. *Appl Mech Mater* 624:249–254. <https://doi.org/10.4028/www.scientific.net/AMM.624.249>
- Khan AR, Rahman MM, Kadrigama K, Ismail AR (2012) RSM model to evaluate material removal rate in EDM of Ti-5Al-2.5Sn using graphite electrode. *IOP Conf Ser Mater Sci Eng* 36:012–016. <http://iopscience.iop.org/1757-899X/36/1/012016>
- Hascalik A, Caydas U (2007) Electrical discharge machining of titanium alloy (Ti–6Al–4V). *Appl Surf Sci* 253(22):9007–9016. <https://doi.org/10.1016/j.apsusc.2007.05.031>
- Ho KH, Newman ST (2003) State of the art electrical discharge machining (EDM). *Int J Mach Tools Manuf* 43(13):1287–1300. [https://doi.org/10.1016/s0890-6955\(03\)00162-7](https://doi.org/10.1016/s0890-6955(03)00162-7)
- Wang YK, Geng XS, Wang ZL, Shan DB (2011) Experimental study of titanium alloy micro-holes by EDM fuzzy control system. *Adv Mat Res* 188:195–198. <https://doi.org/10.4028/www.scientific.net/AMR.188.195>
- Tsai MY, Fang CS, Yen MH (2018) Vibration-assisted electrical discharge machining of grooves in a titanium alloy (Ti-6Al-4V). *Int J Adv Manuf Technol*. <https://doi.org/10.1007/s00170-018-1904-2>
- Yu Z, Zuo DW, Sun YL, Li GH, Chen XM, Zhao JS, Shi KB (2021) Study on the improvement of the surface integrity and efficiency of electrical-discharge-machined TC4 titanium alloy via abrasive flow machining. *Proc Inst Mech Eng Pt B J Eng Manufact* 235(6-7):1197–1211. <https://doi.org/10.1177/0954405420971097>
- Gu L, Li L, Zhao WS, Rajurkar KP (2012) Electrical discharge machining of Ti6Al4V with a bundled electrode. *Int J Mach Tools Manuf* 53(1):100–106. <https://doi.org/10.1016/j.ijmachtools.2011.10.002>
- Wang F, Liu Y, Zhang Y, Tang Z, Ji R, Zheng C (2014) Compound machining of titanium alloy by super high speed EDM milling and arc machining. *J Mater Process Technol* 214(3):531–538. <https://doi.org/10.1016/j.jmatprotec.2013.10.015>
- Zhou M, Meng XY, Qin JJ, Chen ZG, Lian XJ (2013) Building an EDM process model by an instrumental variable approach based on two interactive Kalman filters. *Precis Eng* 37(2013):146–158. <https://doi.org/10.1016/j.precisioneng.2012.07.011>
- Klocke F, Mohammadnejad M, Holsten M, Ehle L, Zeis M, Klink A (2018) A comparative study of polarity-related effects in single discharge EDM of titanium and iron alloys. *Procedia CIRP* 68:52–57. <https://doi.org/10.1016/j.procir.2017.12.021>
- Chen SL, Yan BH, Huang FY (1999) Influence of kerosene and distilled water as dielectrics on the electric discharge machining characteristics of Ti–6Al–4V. *J Mater Process Technol* 87:107–111. [https://doi.org/10.1016/S0924-0136\(98\)00340-9](https://doi.org/10.1016/S0924-0136(98)00340-9)
- Zhou M, Han FZ, Wang YX, Soichiro I (2009) Assessment of dynamical properties in EDM process-detecting deterministic nonlinearity of EDM process. *Int J Adv Manuf Technol* 44:91–99. <https://doi.org/10.1007/s00170-008-1817-6>
- Zhou M, Han FZ, Soichiro I (2008) A time-varied predictive model for EDM process. *Int J Mach Tools Manuf* 48:1668–1677. <https://doi.org/10.1016/j.ijmachtools.2008.07.003>
- Ljung L (1999) System identification—theory for the user, second ed. Prentice-Hall PTR, pp 204–205

Publisher’s note Springer Nature remains neutral with regard to jurisdictional claims in published maps and institutional affiliations.

Springer Nature or its licensor (e.g. a society or other partner) holds exclusive rights to this article under a publishing agreement with the author(s) or other rightsholder(s); author self-archiving of the accepted manuscript version of this article is solely governed by the terms of such publishing agreement and applicable law.